

# Precise Experimental Investigation of Eigenmodes in a Planar Ion Crystal

H. Kaufmann,<sup>1</sup> S. Ulm,<sup>1</sup> G. Jacob,<sup>1</sup> U. Poschinger,<sup>1</sup> H. Landa,<sup>2</sup> A. Retzker,<sup>3</sup> M.B. Plenio,<sup>4</sup> and F. Schmidt-Kaler<sup>1</sup>

<sup>1</sup>*QUANTUM, Institut für Physik, Universität Mainz, Staudingerweg 7, 55128 Mainz, Germany*

<sup>2</sup>*Raymond and Beverly Sackler School of Physics and Astronomy, Tel-Aviv University, Tel Aviv 69978, Israel*

<sup>3</sup>*Racah Institute of Physics, The Hebrew University of Jerusalem, Jerusalem 91904, Givat Ram, Israel*

<sup>4</sup>*Institut für Theoretische Physik, and Center for Integrated Quantum Sciences and Technology, Universität Ulm, Albert-Einstein-Allee 11, 89069 Ulm, Germany*

(Dated: October 24, 2018)

The accurate characterization of eigenmodes and eigenfrequencies of two-dimensional ion crystals provides the foundation for the use of such structures for quantum simulation purposes. We present a combined experimental and theoretical study of two-dimensional ion crystals. We demonstrate that standard pseudopotential theory accurately predicts the positions of the ions and the location of structural transitions between different crystal configurations. However, pseudopotential theory is insufficient to determine eigenfrequencies of the two-dimensional ion crystals accurately but shows significant deviations from the experimental data obtained from resolved sideband spectroscopy. Agreement at the level of  $2.5 \times 10^{-3}$  is found with the full time-dependent Coulomb theory using the Floquet-Lyapunov approach and the effect is understood from the dynamics of two-dimensional ion crystals in the Paul trap. The results represent initial steps towards an exploitation of these structures for quantum simulation schemes.

PACS numbers: 37.10.Ty; 03.67.Lx; 45.50.Jf

Accurate control of ion crystals is of major importance for spectroscopy, quantum simulation, or quantum computing with such experimental platform. Since the invention of dynamical trapping by Paul [1], this versatile instrument has been adapted and optimized for specific purposes. Charged particles, more specifically singly charged ions, are confined in a radio frequency (rf) potential, which is formed by tailored electrode structures. In the case of the linear Paul trap, one aims for a quadrupole field along one  $z$  axis, such that a harmonic pseudopotential in  $x$  and  $y$  direction is formed. This radial potential strongly confines the ions, while an additional weaker axial potential in  $z$  direction is generated with static (dc) voltages applied to end cap electrodes. Trapped ions are cooled by laser radiation [2] in the potential described by three trap frequencies  $\omega_{x,y,z}$  eventually forming a crystallized structure.

The conditions of operation are characterized by two anisotropy parameters where the radial confinement  $\omega_{(x,y)}$  typically exceeds the axial dc confinement  $\omega_z$ . For sufficiently small values of  $\alpha_{(x,y)} \equiv \omega_z^2/\omega_{(x,y)}^2$ , the ion crystal is linear and aligned along the weakest axis, the  $z$  trap axis; all ions are placed in the node of the rf potential. Spectacular highlights using linear crystals of cold ions are the demonstration of quantum logic operations [3, 4], the generation of entangled states [5, 6], sympathetic cooling of ions of different species [7, 8], or the quantum-logic clock [9]. To reach the level of quantum control, as required in the experiments listed above, the first precondition was a complete understanding of eigenmodes and eigenfrequencies for such stored linear ion crystals [10–12].

For larger numbers of ions, or for larger values of  $\alpha$ , the linear crystal undergoes a transition to a zigzag struc-

ture and eventually to a fully crystalline two- or three-dimensional structure [13, 14]. Especially interesting are planar ion crystals, where usually one of the confining radial potentials is much tighter than the axial one, as such structures with nondegenerate radial frequencies do not rotate [15, 16] and allow to address and observe individual ions. Recent proposals have outlined how to achieve laser-induced spin-spin interactions on such 2D ion crystals and how to use their spatial arrangement for the realization of spin lattices exhibiting frustration [17, 18]. It was also proposed how to study the spin-phonon interactions coupling the geometric structure of the ion chain to the spin-spin interaction of the chain to realize a Peierls instability [19] or the Jahn-Teller quantum phase transition [20, 21]. Topological defects in the zigzag configuration were proposed for simulation of quantum effects with solitons [22]. It was also proposed that the dynamics of the structural transition from linear to zigzag configuration may be induced by electronic excitations or a fast change of the trap parameters [23–26] and it would allow for the verification of the predicted scaling laws for defect formation when traversing the transition, that is the Kibble-Zurek mechanism [27, 28]. Furthermore, the double well structure realized by the two different configurations of the zigzag ion crystals can be manipulated and may, thus, allow for the creation of a coherent superposition between these two configurations and hence, serve as a test bed for decoherence models [23, 29].

Spectroscopy and quantum simulation experiments with planar ion crystals in Penning traps have recently been reported [30, 31]. However, no experiments have been successful in using planar crystals in a Paul trap. This is due to the high complexity of controlling such crystalline twodimensional structures. Required is the

knowledge of eigenmodes and eigenfrequencies of such crystals, since it is important for the cooling and for the design of ion-ion interactions which rely on the setting of laser parameters. These are tailored to induce spin-dependent light forces via Stark effects [30, 32, 33].

Here, we present a combined experimental and theoretical study of eigenmodes of ions in planar crystals. We describe an accurate experimental determination of positions of ions and the frequencies of the eigenmodes of the crystal structures together with a comparison of these data with theoretical expectations based on pseudopotential approximation (PPT) and a full dynamical classical theory for solving the linearized Coulomb problem in ion crystals using a Floquet-Lyapunov approach (FLT) [34, 35]. From observations of multiple sequential phase transitions between different structures of the ion crystal, we map out the phase diagram and find good agreement with theoretical predictions following PPT for both the transition points and for the positions of individual ions in the different phases. The measurement of the eigenfrequencies relies on sideband spectroscopy and is applied here to the vibrational frequencies of a three-ion zigzag crystal. Surprisingly, some modes exhibit a significant 37 kHz deviation when compared to calculations in PPT. We can understand the measured data quantitatively only if the full time-dependent solution of the trapping potential is taken into account, with the eigenfrequencies calculated using FLT.

The positions of the ions in a crystal are determined by the mutual Coulomb repulsion together with a static electric potential in the  $z$  direction and a dynamic radial trapping potential. A single charged particle in the time-dependent potential of a quadrupole Paul trap, or the center-of-mass (c.m.) modes of a general crystal of ions, obey decoupled, linear Mathieu equations of motion in each spatial direction [36]. The rf and dc trap voltages, together with the rf-frequency  $\Omega$  and the mass of the ions  $m$ , determine the dimension-free Mathieu parameters in each direction of space  $i \in \{x, y, z\}$  as  $a_i = 4eU_{DC}/\gamma_i m \Omega^2$  and  $q_i = 2eU_{RF}/\gamma'_i m \Omega^2$ , where  $\gamma_i$  and  $\gamma'_i$ , where  $\gamma_i$  and  $\gamma'_i$  are geometrical factors denoting the curvature of the respective potentials and  $\xi = \Omega t/2$ . The Mathieu equation is solved

$$\frac{d^2 y}{d\xi^2} + [a - 2q \cos(2\xi)]y = 0. \quad (1)$$

One derives stable solutions with characteristic exponents  $\beta_i \approx \sqrt{a_i + q_i^2}/2$ , and obtains a harmonic time-independent pseudopotential with frequencies  $\omega_i = \beta_i \Omega/2$ .

In the pseudopotential approximation, the ions arrange in positions corresponding to a stable minimum of the time-independent potential, the determination of which follows the method for linear crystals [10], extending it to three dimensions. In the time-dependent potential, the equivalent of a minimum configuration crystal is a peri-

odic solution with the ions oscillating at the rf-frequency  $\Omega$ , about well-defined average locations (the oscillation denoted as micromotion). The ion coordinates in the radial direction obey

$$y_n(t) = \bar{y}_n \left[ 1 - \frac{q_y}{2} \cos(\Omega t) \right] + \mathcal{O} \left( \frac{q_y^2}{4} \right), \quad (2)$$

while in the axial  $z$  direction, the micromotion is negligible [34].

In the experiment, the resonance fluorescence of Doppler cooled  $^{40}\text{Ca}^+$  ion crystals near 397 nm is imaged on a CCD camera [37]. We use a linear Paul trap consisting of four cylindrical rods ( $2 \times$  rf and  $2 \times$  dc, of diameter 2.5 mm and at diagonal distance between centers of 4.7 mm), and two end caps at 10 mm distance. Note that the degeneracy of the radial modes is lifted using a dc offset voltage of about 0.5 V. We operate with a rf amplitude of  $U_{RF} \sim 300$  V<sub>pp</sub> at  $\Omega/(2\pi) = 14.62$  MHz and end cap voltages of 350 V, yielding secular frequencies  $\omega_{y,z}/(2\pi) = (316, 111)$  kHz and a much larger  $\omega_x$ . All secular frequencies are determined from the resonant electric excitation of the c.m. modes [38].

*Equilibrium positions.*—Are determined from CCD images such as shown in Fig. 1 with a 7-ion crystal. Averaging over 100 exposures and applying a Gaussian fit to the data, we determine the ion locations, see Fig. 1(b). As the planar crystal is observed at an angle of  $45^\circ$ , the  $y$  axis is compressed by  $\sqrt{2}$ . The magnification of the imaging system is determined from the c.m. mode frequency in  $z$  direction and the  $z$  distance in a linear two-ion crystal. The observed fluorescence precisely indicates the ion positions. The measured data show perfect agreement with the theoretical expectations following PPT at the level of a few parts in  $10^5$ , see Fig. 1(c), for a crystal of 7 ions, and similar agreement is found for crystals with 6 to 17 ions.

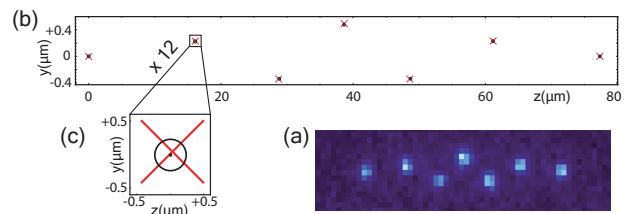


FIG. 1. (color online). Determination of ion positions in planar crystals: (a) The ion fluorescence near 397 nm is imaged on a CCD chip. (b) The ion positions (black dots) are determined by averaging over 100 exposures and compared with the result of a numerical simulation assuming Coulomb repulsion in a harmonic trap pseudopotential (red crosses). The experimental data allow for a precision of 50 nm as indicated by the circle for a  $1 \sigma$  standard deviation.

*Structural phase transitions.*—Are induced when the value of  $\alpha$  is varied. While so far the first linear-to-zigzag

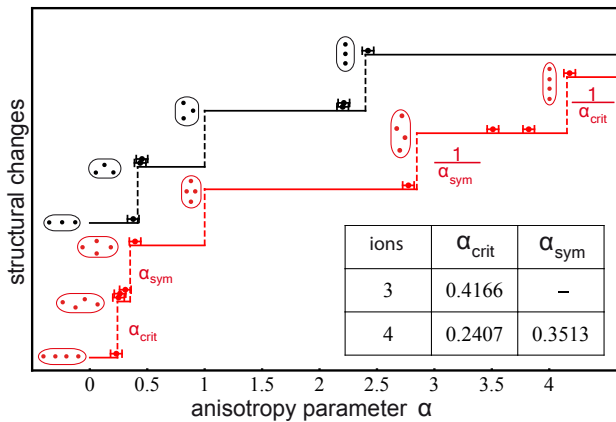


FIG. 2. (color online). Phase transitions for a three-ion (black) and a four-ion (red) crystal. Theoretical (PPT) critical  $\alpha$ 's are indicated by vertical dashed lines with the corresponding crystal configurations. Experimental data are plotted at those  $\alpha$  where a certain configuration is observed, with an error of 0.05 in  $\alpha$ . For an ion crystal with an even number of ions (here,  $N=4$ ),  $\alpha_{\text{sym}}$  is the relevant parameter, where the structure symmetry changes. The measurements are taken in a linear micro trap with  $\Omega/(2\pi) = 22.7$  MHz,  $U_{\text{RF}} \sim 300$  V<sub>pp</sub> yielding frequencies  $\omega_{\{y,z\}}/(2\pi) = (0.421, 0.626)$  MHz and a much larger  $\omega_x$ . Inset: Table of calculated critical  $\alpha$ .

transition was investigated [39], we observe multiple consecutive critical  $\alpha$ , see Fig. 2. The experimentally determined positions and the critical values of  $\alpha$  agree with the prediction of PPT. Comparing the PPT prediction and the solution of the full time-dependent equations, with  $q \lesssim 0.1$ , the relative differences for critical  $\alpha$  are only about 1%, not resolved in the experimental data.

*Normal mode frequencies.*—Result from the Coulomb forces between ions at their equilibrium positions. For the calculation in PPT, these forces are expanded in small excursions about the equilibrium positions, linearized, and the Hessian matrix is solved. Laser spectroscopy provides a precise tool to determine eigenfrequencies with a relative accuracy of 0.2 percent or better, and we do not find agreement between the measurements and the PPT calculation. The corresponding values for mode frequencies for the three-ion crystal under study, in a zigzag configuration with  $\alpha \approx 0.53$ , are in Table I. Only recently, the influence of micromotion on the frequencies of secular modes has been investigated theoretically, which results in significant corrections as compared to PPT, even for relatively small  $q$  values.

Table I displays the resulting frequencies of the  $zz$  modes. Experimental uncertainties result from fluctuations of the trap control voltages, drifts of the laser reference cavity, or magnetic field noise during the scan. We obtain the errors from a statistics of a comparison of red and blue sideband frequencies in many scans like that plotted in Fig. 3, obtained on the same day and under identical conditions as the data. The PPT pre-

TABLE I. Frequencies of a three-ion zigzag crystal in units of  $\text{kHz}/(2\pi)$

	$\omega_{zz(b)}$	$\omega_{zz(a)}$	$\omega_z$	$\omega_y$
Exp.	714(2)	1078(2)	1238(2)	1695(3)
PPT	730(14)	1041(12)		
FLT	715.1	1078.5	1239.5	1690.7

diction for the  $zz$  frequencies is calculated based on the experimental data for the  $\omega_{z,y}$  which are c.m. modes (whose frequencies are the same in PPT approximation and full dynamic theory). Systematic errors, including the ac Stark effect  $<1$  kHz, are contained in the error budget. From the  $z$  and  $y$  mode frequencies, we first determine the ion positions in the pseudopotential and then the  $zz$  mode frequencies. Experimental uncertainties in  $\omega_z$  and  $\omega_y$  lead to uncertainties for the PPT zigzag mode frequency prediction of 14 and 12 kHz, respectively. Theory values for FLT are obtained as a best fit to all experimentally determined frequencies [40].

The breakdown of PPT results from the fast oscillations of ions about their equilibrium positions at the rf-frequency, as in Eq. (2), which modifies periodically the Coulomb forces between ions. Thus, it is not justified to assume static positions for the Hessian matrix. The forces between the ions can be expanded in a Fourier series, and the resulting equations can be solved in terms of decoupled modes [34], which describe oscillations with secular frequencies, superimposed on micromotion at the rf-frequency. This effect resembles the Lamb shift where the Zitterbewegung of the bound electron leads to a modification in the hydrogen energy levels [41]. A short description of the method of solution, together with code for the calculations presented in this Letter, is available in the Supplemental Material [40].

We test the FLT prediction experimentally using a threeion crystal and performing resolved sideband spectroscopy on the narrow  $S_{1/2}$  to  $D_{5/2}$  transition near 729 nm. In the spectrum (Fig. 3), we identify the vibrational frequencies of a three-ion zigzag crystal. When testing PPT, we use the c.m. modes in axial and radial  $y$  direction to generate predictions for the zigzag frequencies, which deviate from the experimental values by 37 and 15 kHz, respectively. For FLT, we fit the five measurements of the three c.m. modes and the two lowest planar zigzag modes using a weighted-least-squares fit, with three parameters  $q_y$ ,  $a_z$  and  $a_y$  (imposing  $a_x = -a_z - a_y$  as required from the Laplace equation). The weighted-least-squares fit norm is a random variable distributed like  $\chi^2$  with two degrees of freedom, see Ref. [40]. The theoretical values coincide exactly with both the eigenfrequencies, fitting the data with about 22% probability with all the eigenfrequencies. A similar fitting procedure for the PPT results in a negligible probability of the order  $10^{-11}$ , reflecting that PPT frequencies

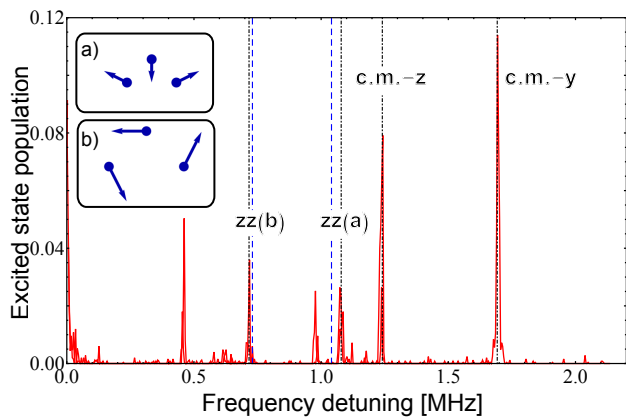


FIG. 3. (color online). Spectrum of vibrational modes in a three-ion crystal. The excitation from the  $S_{1/2}$  to  $D_{5/2}$  state is plotted as the laser frequency near 729 nm is scanned over the resonance between a frequency detuning of  $\pm 2$  MHz. We observe excitation at the frequencies of red and blue motional sidebands, symmetrical around the carrier. The spectrum is plotted versus the modulus of frequency detuning, such that red and blue sidebands fall on each other. Measurements are taken in a linear micro trap with  $\Omega/(2\pi) = 35.07$  MHz and  $U_{\text{RF}} \sim 420 V_{\text{pp}}$  yielding frequencies  $\omega_{\{x,y,z\}}/(2\pi) = \{2940(10), 1695(3), 1238(2)\}$  kHz. We identify zigzag modes near (a) 1078(2) kHz and (b) 0.714 (2) kHz. The blue dashed lines indicate the expected frequencies for zigzag modes from PPT, while the black dashed-dotted lines show the outcome of the calculation of FLT. Insets display eigenvectors of zigzag modes (a) and (b). The other resonances correspond to mixing frequencies of two normal mode frequencies.

do not agree with the experimental finding.

The strong influence of the trap drive on the eigenfrequencies of zigzag modes is further explained by a theoretical analysis, where the Mathieu parameter  $q$  is varied and the variation of the mode frequencies  $zz(a)$  and  $zz(b)$  is plotted, see Fig. 4. In the experiment, the  $q$  value is fixed and can not varied easily over a large range. The data points, near  $q = 0.2$ , for the  $zz(a)$  and  $zz(b)$  mode, hit the FLT prediction and exclude the PPT frequencies. The fractional frequency shift reaches, for high  $q$  values, a level of up to 20%. Examining Fig. 3(a), it is understandable why the  $zz(a)$  mode is affected the most by the micromotion, and why its frequency increases monotonically with  $q$ . It can be seen from Eq. (2) that the micromotion amplitude of each ion is proportional to the negative of its  $y$  equilibrium position, so that this motion has a large projection on the eigenvector of the  $zz(a)$  mode. At each point along the periodic trajectory, the restoring forces are larger for this mode than at the center, and thus, its frequency increases with the amplitude of the micromotion, hence, with  $q$ .

*Conclusion.* — We calculated and characterized experimentally the behavior of two-dimensional crystals under the influence of micromotion. We show that while

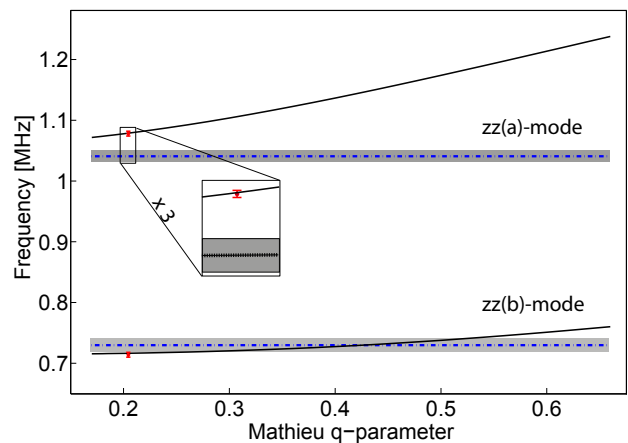


FIG. 4. (color online) The calculated eigenfrequencies for the zigzag modes (a) and (b) in a three-ion crystal plotted versus the Mathieu parameter  $q$ , with  $a$ -parameters adjusted such that the c.m. frequencies are constant. The  $zz$  eigenfrequencies show a slope with  $q$ . The dashed line results from the PPT, see Table I, including the prediction error (grey shaded). Experimental data point fit the theoretical FLT expectation near  $q \approx 0.2$ , where  $\Omega/(2\pi)$  equals 35.07 MHz. Inset: with zoomed part showing the fit of the FLT and the  $3\sigma$  deviation of data against PPT.

the pseudopotential theory fails to explain the experimental results to an accuracy within  $3\sigma$ -deviation, the newly established method predicts the experimental finding correctly. We could show that FLT provides an experimentally verified tool for understanding the static and dynamic properties of mesoscopic Coulomb crystals and might prove to be a key ingredient for establishing these systems as a new experimental platform. The presented results are an essential prerequisite for the success of quantum simulation in two-dimensions where the effective Hamiltonian depends on the crystal frequencies of all normal modes in the presence of micromotion.

It is important to note that micromotion is a driven motion with a well-defined phase: Therefore, it does not delocalize the ion wave packet, leading to a larger effective Lamb Dicke parameter. The micromotion merely acts as to affect the strength of atom-laser interactions via phase modulation. It does not prevent from exploiting spin dependent forces for quantum simulation schemes.

Based on our results, a theory could be constructed that takes into account such effects in the effective Hamiltonian. Moreover, the precise knowledge of the behavior of the crystal under the influence of micromotion is crucial for quantum-to-classical simulation experiments that use such transitions in condensed matter or high energy effects, such as the Kibble Zurek mechanism. The deviation of critical  $\alpha$  values from the pseudopotential predictions is expected to be larger for larger values of  $q$  and merits further experimental and theoretical investigation.

We acknowledge financial support by the European commission within the Integrated Projects AQUTE and QESSENCE, the EU STREP PICC, the German-Israeli-Foundation and the Alexander von Humboldt Foundation.

- 
- [1] W. Paul and H. Steinwedel, *Z. Naturforsch. Teil A* **8**, 448 (1953).
- [2] D. J. Wineland and H. G. Dehmelt, *Bull. Am. Phys. Soc.* **20**, 637 (1975).
- [3] J. I. Cirac and P. Zoller, *Phys. Rev. Lett.* **74**, 4091 (1995).
- [4] F. Schmidt-Kaler, H. Häffner, M. Riebe, S. Gulde, G. P. T. Lancaster, T. Deuschle, C. Becher, C. Roos, J. Eschner, and R. Blatt, *Nature* **422**, 408 (2003).
- [5] C. Roos, M. Riebe, H. Häffner, W. Hänsel, J. Benhelm, G. P. T. Lancaster, C. Becher, F. Schmidt-Kaler, and R. Blatt, *Science* **304**, 1478 (2004).
- [6] T. Monz, P. Schindler, J. T. Barreiro, M. Chwalla, D. Nigg, W. A. Coish, M. Harlander, W. Hänsel, M. Hennrich, and R. Blatt, *Phys. Rev. Lett.* **106**, 130506 (2011).
- [7] M. Barrett, B. L. DeMarco, T. Schaetz, V. Meyer, D. Leibfried, J. Britton, J. Chiaverini, W. M. Itano, B. M. Jelenkovic, J. D. Jost, C. Langer, T. Rosenband, and D. J. Wineland, *Phys. Rev. A* **68**, 042302 (2003).
- [8] D. J. Larson, J. Bergquist, J. J. Bollinger, W. M. Itano, and D. J. Wineland, *Phys. Rev. Lett.* **57**, 70 (1986).
- [9] P. O. Schmidt, T. Rosenband, C. Langer, W. M. Itano, J. C. Bergquist, and D. J. Wineland, *Science* **309**, 749 (2005).
- [10] D. F. V. James, *Appl. Phys. B* **66**, 181 (1998).
- [11] A. Steane, *Appl. Phys. B* **64**, 623 (1997).
- [12] C. Marquet, F. Schmidt-Kaler, and D. F. V. James, *Appl. Phys. B* **76**, 199 (2003).
- [13] M. Drewsen, C. Brodersen, L. Hornekær, J. Hangst, and J. Schiffrer, *Phys. Rev. Lett.* **81**, 2878 (1998).
- [14] G. Birkl, S. Kassner, and H. Walther, *Nature (London)* **357**, 310 (1992).
- [15] T. Hasegawa and J. J. Bollinger, *Phys. Rev. A* **72**, 043403 (2005).
- [16] J. M. Taylor and T. Calarco, *Phys. Rev. A* **78**, 062331 (2008).
- [17] A. Bermudez, J. Almeida, F. Schmidt-Kaler, A. Retzker, and M. B. Plenio, *Phys. Rev. Lett.* **107**, 207209 (2011).
- [18] A. Bermudez, J. Almeida, K. Ott, H. Kaufmann, S. Ulm, U. Poschinger, F. Schmidt-Kaler, A. Retzker, and M. Plenio, *New J. Phys.* **14**, 093042 (2012).
- [19] A. Bermudez and M. B. Plenio, *Phys. Rev. Lett.* **109**, 010501 (2012).
- [20] D. Porras, P. A. Ivanov, and F. Schmidt-Kaler, *Phys. Rev. Lett.* **108**, 235701 (2012).
- [21] P. A. Ivanov, D. Porras, S. S. Ivanov, and F. Schmidt-Kaler, arXiv:1207.0452 (2012).
- [22] H. Landa, S. Marcovitch, A. Retzker, M. B. Plenio, and B. Reznik, *Phys. Rev. Lett.* **104**, 043004 (2010).
- [23] A. Retzker, R. Thompson, D. Segal, and M. B. Plenio, *Phys. Rev. Lett.* **101**, 260504 (2008).
- [24] S. Fishman, G. De Chiara, T. Calarco, and G. Morigi, *Phys. Rev. B* **77**, 064111 (2008).
- [25] A. delCampo, G. De Chiara, G. Morigi, M. B. Plenio, and A. Retzker, *Phys. Rev. Lett.* **105**, 075701 (2010).
- [26] D. G. De Chiara, A. delCampo, G. Morigi, M. B. Plenio, and A. Retzker, *New J. Phys.* **12**, 115003 (2010).
- [27] T. W. B. Kibble, *J. Phys. A* **9**, 1387 (1976).
- [28] W. H. Zurek, *Nature (London)* **317**, 505 (1985).
- [29] W. Li and I. Lesanovsky, *Phys. Rev. Lett.* **108**, 023003 (2012).
- [30] J. Britton, B. C. Sawyer, A. Keith, C.-C. J. Wang, J. K. Freericks, H. Uys, M. J. Biercuk, and J. J. Bollinger, *Nature (London)* **484**, 489 (2012).
- [31] B. C. Sawyer, J. Britton, A. Keith, C. Wang, J. Freericks, H. Uys, M. Biercuk, and J. Bollinger, *Phys. Rev. Lett.* **108**, 213003 (2012).
- [32] D. Leibfried, B. L. DeMarco, V. Meyer, M. Barrett, J. Britton, W. M. Itano, B. Jelenkovic, C. Langer, T. Rosenband, and D. Wineland, *Nature (London)* **422**, 412 (2003).
- [33] R. Islam, E. E. Edwards, K. Kim, S. Korenblit, C. Noh, H. Carmichael, G.-D. Lin, L.-M. Duan, C.-C. Joseph Wang, J. K. Freericks, and C. Monroe, *Nature Commun.* **2**, 377 (2011).
- [34] H. Landa, M. Drewsen, B. Reznik, and A. Retzker, *New J. Phys.* **14**, 093023 (2012).
- [35] H. Landa, M. Drewsen, B. Reznik, and A. Retzker, *J. Phys. A* **45**, 455305 (2012).
- [36] D. Leibfried, R. Blatt, C. Monroe, and D. J. Wineland, *Rev. Mod. Phys.* **75**, 281 (2003).
- [37] H. C. Nägerl, W. Bechter, J. Eschner, F. Schmidt-Kaler, and R. Blatt, *Appl. Phys. B* **66**, 603 (1998).
- [38] H. C. Nägerl, R. Blatt, J. Eschner, F. Schmidt-Kaler, and D. Leibfried, *Opt. Express* **3**, 89 (1998).
- [39] D. G. Enzer, M. M. Schauer, J. J. Gomez, M. S. Gulley, M. H. Holzscheiter, P. G. Kwiat, S. K. Lamoreaux, C. G. Peterson, V. D. Sandberg, D. Tupa, A. G. White, R. J. Hughes, and D. F. V. James, *Phys. Rev. Lett.* **85**, 2466 (2000).
- [40] See Supplemental Material at <http://link.aps.org/supplemental/10.1103/PhysRevLett.109.263003> for source code files and a description of their content, together with more details of the calculations performed.
- [41] M. Weitz, F. Schmidt-Kaler, and T. W. Hänsch, *Phys. Rev. Lett.* **68**, 1120 (1992).